PHYSOR 2004 -The Physics of Fuel Cycles and Advanced Nuclear Systems: Global Developments
Chicago, Illinois, April 25-29, 2004, on CD-ROM, American Nuclear Society, Lagrange Park, IL. (2004)

Coupled Calculations Using the Numerical Nuclear Reactor for Integrated Simulation of Neutronic and Thermal-Hydraulic Phenomena

D. P. Weber*[1], T. Sofu[1], W. S. Yang[1]
T. J. Downar[2], J. W. Thomas[2], Z. Zhong[2]
H. G. Joo[3]

[1]*Argonne National Laboratory (208), 9700 S. Cass Ave., Argonne, IL 60439 USA*
[2]*Purdue University, 1290 Nuclear Engineering, Building, West Lafayette, IN 47907*
[3]*Korea Atomic Energy Research Institute, Yuseong, Daejeon 305-600, Korea*

The Numerical Nuclear Reactor is a collaborative US-ROK I-NERI project to develop a comprehensive high fidelity reactor core modeling capability for detailed analysis of current and advanced reactor design. High fidelity models of thermal-hydraulics and neutronics have been incorporated into the initial version of the integrated code. Computational fluid dynamics (CFD) methods, based on the STAR-CD commercial CFD code, are used for the thermal-hydraulic analysis, while neutronics calculations are being performed with the whole core discrete integral transport code, DeCART. A robust coupling strategy for integrated, high-fidelity thermal-hydraulic/neutronic calculations has been developed. Examples of the coupled code analysis capability are provided for single pin, multi-pin and mini-core configurations, as well as estimates of computational requirements for integrated whole core calculations.

KEYWORDS: Thermal-hydraulics, neutronics, coupled codes, computational fluid dynamics, CFD, integral transport theory, reactor physics, core analysis, high performance computing, parallel computers, numerical reactor

1. Introduction

As part of a US-ROK collaborative I-NERI project, a comprehensive high fidelity reactor core modeling capability is being developed for detailed analysis of current and advanced reactor designs. The work involves the coupling of advanced numerical models such as computational fluid dynamics (CFD) for thermal hydraulic calculations, whole core discrete integral transport for neutronics calculations, and thermo-mechanical techniques for structural calculations.

Previous papers have provided an overview of the project [1,2] and detailed discussions of the key phenomenological models and the interfaces for the coupling of these models. In this paper, attention is focused on the results obtained using the coupled code, the primary objective of the project. As noted in papers on code interfaces and numerical iteration strategies [3,4], techniques for coupling the reactor physics module, DeCART, to the CFD thermal-hydraulics module, STAR-CD, have been demonstrated. This coupling between the reactor physics module

* Corresponding author: Tel. 630-252-8175, FAX 630-252-5318, E-mail: dpweber@anl.gov

and the CFD module has been developed to be a generic coupling. Although the initial coupling has focused on coupling DeCART to the STAR-CD [5] CFD code, coupling to other CFD capabilities is expected to be straightforward. The project team at KAERI, in fact, is utilizing the interface routines to couple the CFD-ACE code [6] to DeCART.

Three key steps in coupled calculations are:

- mapping of the CFD mesh (cells) onto the neutronics mesh (zone set) for coupled calculations,
- volume averaging of the temperature and density distributions over the CFD cells in each zone before transferring them to DeCART,
- reverse-mapping of the zone based volumetric heat generation rates from the neutronics component onto the CFD mesh.

The associations between the CFD mesh and the neutronics zone set for mapping and reverse-mapping are established during the model development phase; therefore, it does not constitute an overhead during coupled calculations. However, the volume averaging of the state variables needs to be performed during each data exchange cycle.

The coupled calculations start with a converged flow solution obtained with a stand-alone STAR-CD run based on a prescribed volumetric heat generation rate in the fuel. With a STAR-CD user subroutine, the calculated cell temperatures and coolant densities are transferred to the interface module. After receiving this data set, the interface module calculates volume based averages for temperatures and coolant densities in each zone, calculates the norm of matrix for enthalpy and power density residuals (to monitor convergence), and transfers them to DeCART. When the DeCART calculations are completed, the zone based volumetric heat generation rates are transferred to STAR-CD via the interface.

In the current implementation, the STAR-CD and DeCART codes run sequentially. There are three important convergence criteria: (1) STAR-CD local convergence, determined by the enthalpy residual; (2) DeCART local convergence, determined by its own set of residuals; and (3) The interface power residual, which is based on the difference in power distribution from data exchange to data exchange. The coupled calculations are flagged as converged only when all of these criteria have been satisfied.

In this paper, we describe the results of a series of sample problems performed with the coupled code. These sample problems include single pin calculations, a small test problem involving a 3x3 matrix of pins of varying compositions, and a so-called mini-core problem consisting of four quarters of neighboring subassemblies. Estimates of computational requirements for a large core problem consisting of several subassemblies representing $1/8^{th}$ of a symmetric core are also provided.

2. Single Pin Model

To establish an effective coupling strategy, initially a steady-state single-pin analysis was considered assuming symmetry boundary conditions (infinite array of pins). To assure consistent data exchange on a common grid, the fuel pin is discretized into explicit representation of fuel pellets with several radial rings, the cladding, and the coolant volumes. Each of these volumes is further subdivided into 8 azimuthal segments, and 20 axial segments as shown in Fig. 1 with orange colored lines. Thus, a single fuel pin is represented with 6x8x20=960 zones on which the

volume averaged temperatures and heat generation rates are specified and exchanged between the CFD and neutronics components. As shown in Fig. 1, the CFD calculations are performed on a more refined mesh structure than the zone structure defined above. The CFD models used for single-pin simulations included a few hundred thousands of computational cells.

The importance of coupling a detailed thermal-hydraulic analysis to the reactor physics analysis was demonstrated by comparing the effect of space dependent self-shielding on Doppler reactivity for a single mixed-oxide (MOX) fuel pin. In this case, a 2-D version of the DeCART code was used and the temperature distribution was determined analytically to provide "ring-wise" feedback effects in the fuel. Infinite multiplication factor, k_∞, and Doppler reactivity comparisons were made with respect to the standard method based on the average temperature for the whole pin. The results shown in Table 1 illustrate a 27% difference in Doppler reactivity worth when average fuel pin temperatures are used, and a 9% difference even when the current practice of using an "effective temperature" based on centerline and surface temperatures are used, consistent with the observations of Takeda, et al.[7].

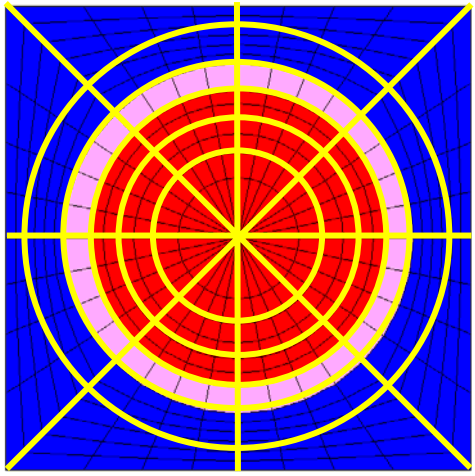

Fig.1 The CFD Mesh (black lines), The Zone Set Boundaries for Coupled Calculations (yellow lines).

Table 1 Single-Pin Test Problem: Effect of Space Dependent Self-Shielding on Doppler Reactivity

	Calculated k_∞			
Power density (W/cm^3)	With Distributed temperatures	With Average temperature	With Effective temp.with β=0.3	Effective temp. with β=0.242
177	1.38123	1.37926	1.38070	1.38122
224	1.37898	1.37641	1.37825	1.37893
Reactivity difference (pcm)	118.1	150.1	128.7	120.2
Relative error (%)	--	27%	9%	<2%

3. Multi-pin Model

Further testing of the coupled calculations has been done on models of 3x3 pin arrays as shown in Figure 2. This small model consists of five UO_2 pins, three MOX pins, and a central guide tube. Details of the model discretization are provided in Table 2 and the constant thermophysical properties used are summarized in Table 3. An inlet boundary condition of a 1 m/s uniform flow of 543 K water with a turbulent intensity of 0.2 is specified with a total assembly power of 1.626×10^5 W. Solid surfaces at the inlet and outlet planes are considered adiabatic. All other vertical surfaces are assigned symmetry boundary conditions. The DeCART model includes reflector regions at the top and bottom, which are not modeled in STAR-CD. These regions consist only of water and cladding. In the absence of gamma heating, these regions generate no power; therefore, they are assumed to have the same temperatures and densities of those in the adjacent layers.

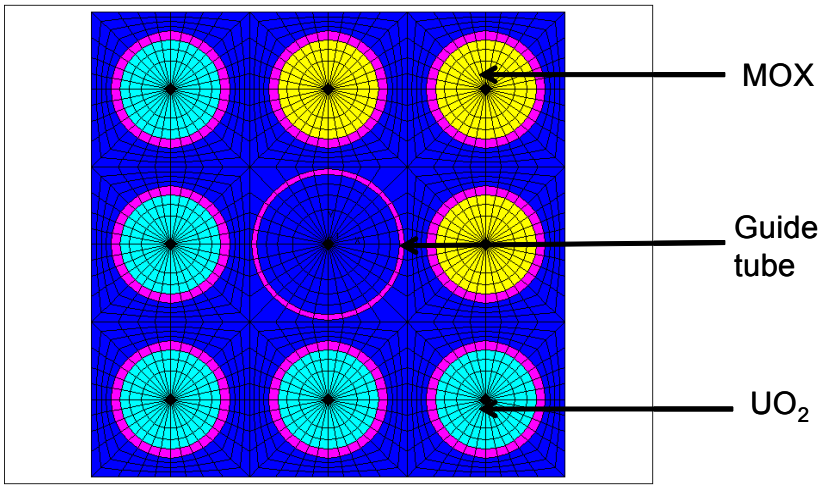

Fig.2 UO_2/MOX 3x3 Geometry

Table 2 3x3 Model Discretization

	STAR-CD	DeCART
Fuel Pins		
Fuel rings	3	3
Clad rings	1	1
Coolant rings	4	2
Azimuthal slices	32	8
Axial planes	500	10 (12)
Guide Tube		
Inner coolant rings	4	4
Clad rings	1	1
Outer coolant rings	1	1
Azimuthal slices	32	8
Axial planes	500	10 (12)
Total number of cells/zones	1.12e+6	5184

Table 3 Thermophysical Properties, All Are Constant

Material	Density (kg/m^3)	Conductivity (W/m-K)	Specific Heat (J/kg-K)	Viscosity[a] (kg/m-s)	Pressure (Pa)
Water	0.775e+3	0.575	5000	1.e-4	1.5e+7
UO_2	11e+3	6	300	-	-
MOX	11e+3	5	300	-	-
Clad	6.5e+3	17	350	-	-

(a) Viscosity is molecular (not turbulent) and the pressure listed is the monitoring pressure

The coupled solution for the mid-plane temperature distribution is shown in Figure 3. The figure shows the expected asymmetry caused by the different kinds of pins. The corner MOX pin is cooler than surrounding MOX due to its comparatively lower moderation. A significant azimuthal variation in temperature within the fuel is also noted, possibly exaggerated by the lack of azimuthal dependence on cross sections in DeCART.

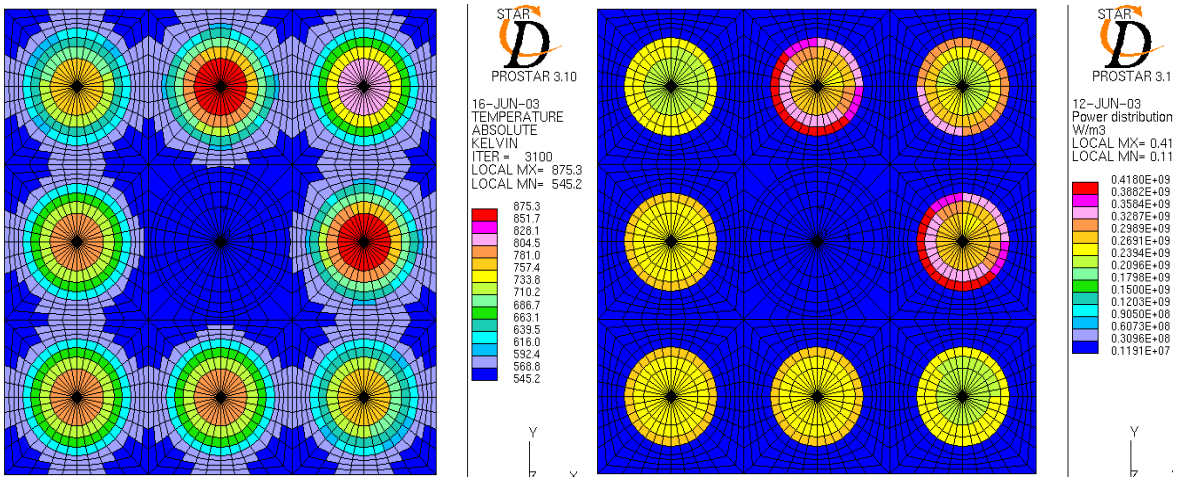

(a) Mid-plane temperature distribution (b) Mid-plane power distribution.

Fig.3 Results for UO_2/MOX assembly.

An assessment of the impact of CFD discretization on the accuracy and cost of coupled calculations was conducted with the 3x3 multi-pin model using 16 different mesh configurations. Four different radial mesh structures with 3, 6, 9, and 12 equal-area rings were considered for the fuel. The cladding was represented as a single layer, and the coolant was considered with four rings in radial direction. Two azimuthal discretization options with 24 and 32 slices were studied. In axial direction, two configurations with 300 and 500 layers were considered. In all cases, the same DeCART model with over 5000 neutronic zones was used (three rings in each fuel, one in cladding, and two in coolant, eight azimuthal slices, and 10 axial layers along the active core height). All characteristics related to coupling, including decomposition and data exchange frequency, were fixed for all cases.

The most significant impact on run time is axial mesh. For the case with 6 rings and 32 slices, the run time jumps 136% when moving from 300 to 500 axial mesh. The azimuthal dependence on run time is also found to be significant. Although increase in elapsed time is proportional with number rings in fuel for $r \leq 9$, there is a significant difference between the cases with 9 and 12 rings in the fuel. The memory requirement is again most strongly affected by the number of axial mesh. The infinite multiplication factor depends primarily on azimuthal discretization with approximately 50 pcm difference between the cases with 24 to 32 azimuthal slice meshes. Only 15 pcm difference is observed when moving for 3 to 6 rings in fuel. Moving beyond 6 rings makes less than a 5 pcm impact. The impact of moving from 300 to 500 axial layers is less than 5 pcm for all cases.

The maximum temperature depends most strongly on radial discretization. The maximum temperature difference is 24 K between the cases with 3 to 12 rings in fuel. However, the difference is only an 8 K between the cases with 6 to 12 rings in fuel. Again, the axial discretization has a negligible impact on maximum temperature. Heat flux does not appear to be influenced significantly by differences in meshing. It should also be noted that the locations of the maximum temperature and heat flux do not change with discretization. Most of the results reported in this paper are performed using a CFD grid with six equal-area rings in the fuel, 24 azimuthal slices, and 300 axial segments.

4.0 Mini-Core Model

To assess the performance of the coupled tool for larger problems, a checkerboard core configuration is also studied. The checkerboard core consists of a repeating array of UO_2 and MOX fuelled assemblies in a cross pattern as shown in Fig. 4. The characteristics for both types of fuel assemblies are summarized in Table 4. With the CFD model, this configuration is represented with two adjacent 1/8 assemblies (one with UO_2 and the other with MOX fuel) as the smallest symmetric segment shown as the enlarged green triangle in Fig. 4. Since only rectangular segments can be simulated with the neutronic module, DeCART, the checkerboard configuration is represented as four quadrants (two with UO_2 and the other two with MOX fuel) shown as the blue square in Fig. 4.

Table 4 Mini-Core Fuel Assembly Specifications

Number of fuels in an assembly	264
Number of guide tubes per assembly	25
Cladding inner radius	0.4189 cm
Cladding outer radius	0.4759 cm
Rod pitch	1.262 cm
Guide tube inner radius	0.5709 cm
Guide tube outer radius	0.6130 cm
Active fuel height	200 cm
Average linear heat generation rate	109.65 W/cm
Average flow rate	0.09446 kg/s
Coolant inlet temperature	270 C
Coolant inlet pressure	150 bar

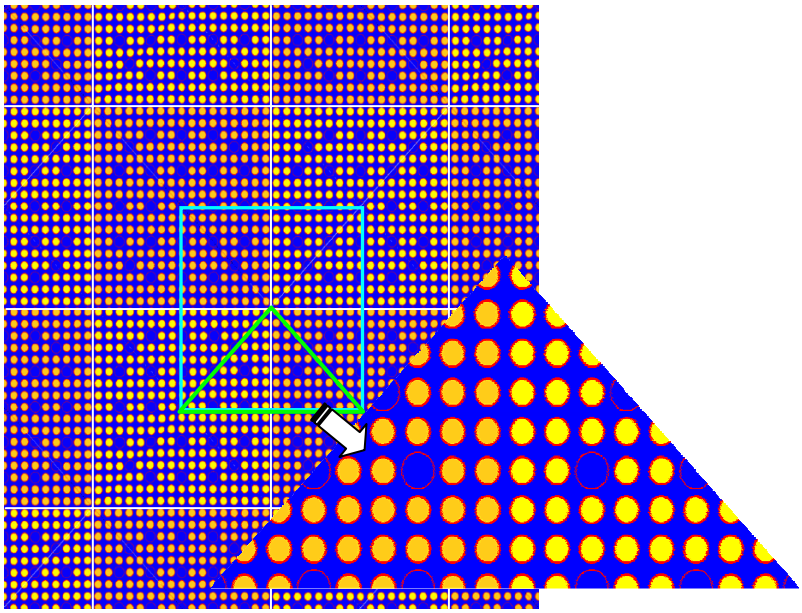

Fig.4 The checkerboard core configuration. The blue square represents the symmetric segment used in the DeCART model; the enlarged green triangle shows the symmetric segment for CFD simulations. The orange color indicates UO_2 fuel pins, the yellow color indicates MOX fuel pins.

The DeCART model for neutronics calculations consists of 5 radial rings (three in the fuel, one in cladding, and one in the coolant zones), 8 azimuthal slices, and 12 axial planes, thus a total of 480 computational zones for each pin. This adds up to a total of 150,000 neutronics zones in four quadrants. The CFD model, on the other hand, has 300 axial layers, 24 azimuthal slices, and 10 rings per fuel pin, of which 6 rings are in the fuel, resulting in a total of about 5 million computational cells (about 1 million of which are fluid cells). To cut down the computation time, the problem is studied in several stages. Initially, a converged flow solution is obtained for the checkerboard core configuration, followed by a second step in which the temperature distributions are determined by solving only for the enthalpy using the flow field obtained in the first step and a cosine shaped power profile in each pin. These initial steps set the stage for the coupled STAR-CD/DeCART calculations that restarts from the converged flow field and a reasonable initial guess for temperature distributions.

Using the stand-alone CFD model, a converged flow solution is obtained and a timing study is completed for checkerboard core configuration with various decomposition options using the *jazz* LINUX cluster at ANL. The statistics are compiled for identical calculations over 100 iterations beginning from the same restart file, and solving all seven field variables with conjugate heat transfer. In addition to the automatic decomposition option based on Metis optimization, the checkerboard core configuration is decomposed manually by defining cell sets containing identical number of fluid and solid cells (Fig. 5). In the first option considered, the computational domain is divided into 25 axial layers with equal-height (1x25 case). In the second option, the computational domain is divided into 12 axial layers with each layer further subdivided into two identical columns—one corresponding to 1/8 UO_2 assembly and the other for 1/8 MOX assembly (2x12 case). In the last option, the computational domain is divided into 6 axial layers, each of which with four symmetric segments—two for UO_2 and another two for MOX assembly (4x6 case). A summary of timing statistics is provided in Table 5.

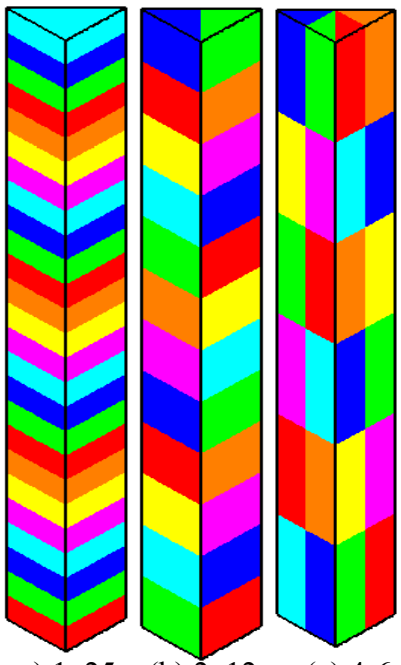

a) 1x25 (b) 2x12 (c) 4-6

Fig.5 Manual Decomposition Options Considered

Table 5 Summary of CFD Timing Statistics for Checkboard Core Configuration with Various Decomposition Options

Decomposition option	Compute nodes	CPU time/ iteration (s)	Elapsed time/ iteration (s)	Total time (min)
Automatic (Metis)	24	12.57±6.16	27.95±12.86	46.6
Automatic (Metis)	25	12.16±6.07	30.48±14.96	50.8
1x25	25	11.10±4.90	30.70±13.62	51.2
2x12	24	9.22±4.08	16.24± 6.33	27.1
4x6	24	8.81±4.34	16.19± 5.94	27.0

The results clearly show that manual decomposition, when based on symmetric regions with equal number cells and minimized surface-to-volume ratio, provide best results in terms of reduced total computation time. Decomposing the domain into symmetric zones with equal

number of cells evens out the CPU time spent for each processor and substantially reduces idling. Minimizing the surface-to-volume ratio reduces the communication overhead between the nodes. The results also show that the decomposition option has no noticeable effect of the rate of convergence of the field variables, i.e., the reduction in residuals after 100 iterations is almost identical for each case.

Sample calculated results with the mini-core model are shown in Figure 6**.** For this run, all properties were constant in STAR-CD, but a temperature-dependent fluid density was simulated by the interface.

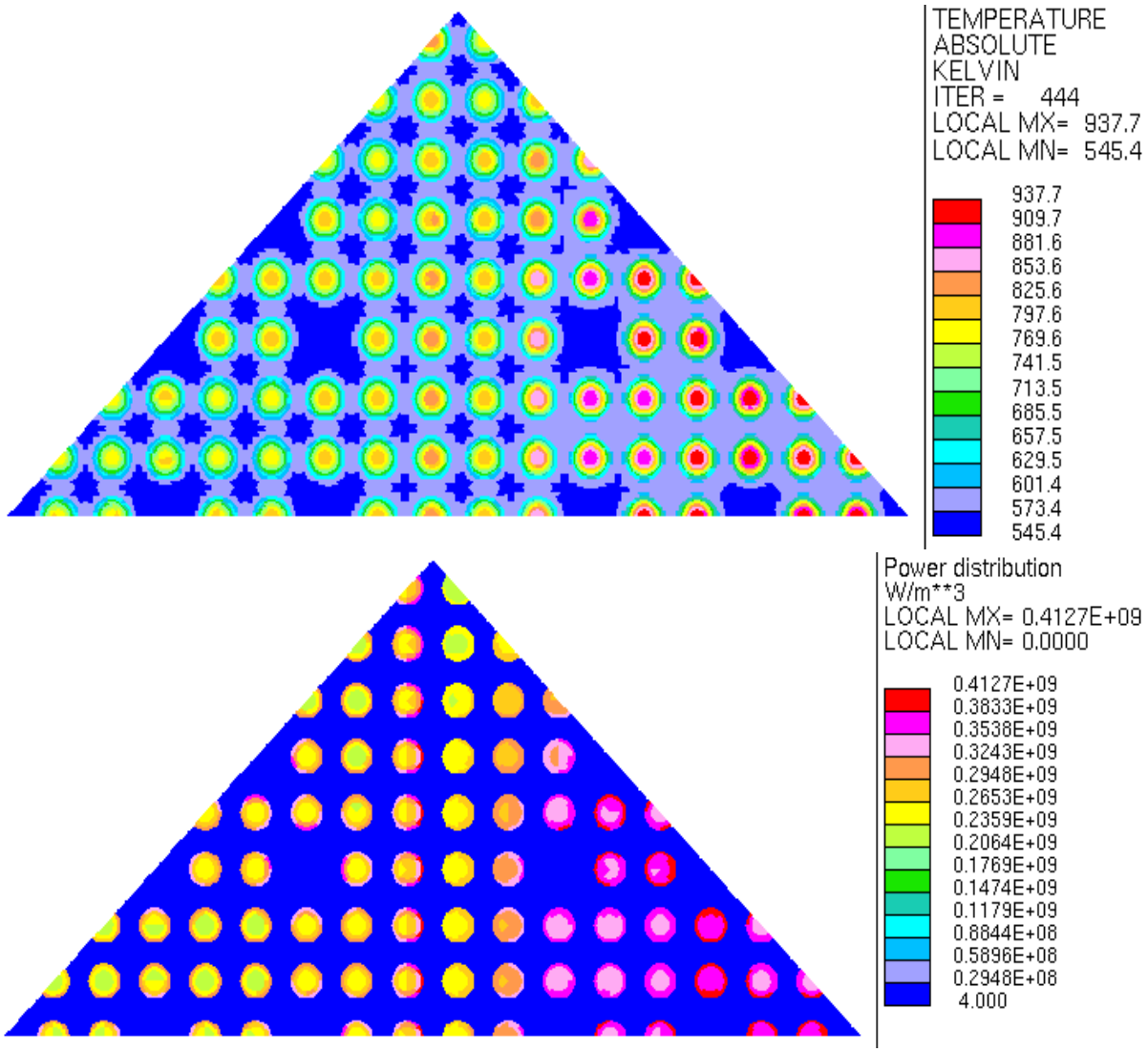

Fig.6 Sample Results for The Mini-Core Problem: Mid-plane Temperature Distribution (top), Mid-plane Power Distribution (bottom).

5.0 Summary and Conclusion

The use of use of coupled, high-fidelity models for reactor physics and thermal-hydraulics illustrates the level of detail and the consistent calculation of feedback effects in such a methodology. Previous detailed thermal-hydraulic analyses using CFD [8] showed consistency

with traditional subchannel codes, such as VIPRE[9], for average effects such as outlet temperatures and average subchannel temperatures. Hot spots close to the fuel pins and the details of asymmetrics within the channel, however, requires this level of higher fidelity analysis. This approach, particularly when coupled to sub-pin level reactor physics models, provides detailed neutronic feedback estimates and local thermal-hydraulic conditions. Such details may be important, for example, in estimating the potential for sub-cooled nucleate boiling, which may have important operational implications, as in the conditions associated with Axial Offset Anomaly [10].

Based on this initial set of coupled calculations, where typical steady state results require several hundred iterations, a preliminary estimate of the amount of computing time for whole core calculations has been made as shown in Table 6. Based on these results, it appears that a complete integrated steady state calculation on a teraflop class machine, such as that available at Argonne, would require 3.3 hours CPU time for a small core with 57 assemblies. In a transient calculation, such as the control rod withdrawal, it is expected that the required real time for analysis will be approximately 10 seconds. With time steps of 10 msec and 10 iterations per transient time step, we are now estimating that such a transient calculation can be performed in a time frame of several tens of hours or a few days on the teraflop class machine. The results of the calculations show scalability with the rated performance of the computational resource, suggesting that steady state and transient calculations with this high fidelity integrated analytical tool will be possible in a matter of hours on machines with ratings 10 to 100 teraflops, which are becoming available commercially today.

Table 6 CPU Time Projections for Large Core Models

		Large PWR	Small PWR
Number of fuel assemblies	Total	193	57
	1/8 model	24 1/8	7 1/8
Total Number of Cells (millions)		480 M	140 M
With 420K cells per processor	# of processors	1150	335
	CPU time	200 min	200 min
With 840K cells per processor	# of processors	575	268
	CPU time	600 min	600 min

Demonstration of the ability to perform whole core steady-state and transient calculations is a primary objective in the third year of this I-NERI project. The completion of the transient analysis capability of DeCART and the results of the investigation of optimal numerical strategies are critical elements of the research program. The results of these near term activities are expected to confirm the required computing time for realistic whole core problems provided in the estimates given above.

The ability to perform such calculations and confidence in the calculated results, however, are two separate issues. As discussed earlier, validation of the individual modules continues to be demonstrated as part of this I-NERI project. Validation of the integrated calculation is an important objective for future work. Specific examples for this validation are being considered and recommendations for future work will be provided. Potential examples include the NEACRP 3-D LWR Core Transient Benchmark and the NEA Pressurized Water Reactor Main Steam Line Break (MSLB) Benchmark. The expectation is that results of these calculations will be generally comparable to other calculated results, but the level of detail provided by this

analysis will be considerably greater. Thus, the expected results will allow us to evaluate the accuracy of traditional methods and their implications on performance and safety.

Acknowledgements

This work was completed under the auspices of the U.S. Department of Energy Office of Nuclear Energy as part of the International Nuclear Energy Research Initiative (INERI) with Republic of Korea. The submitted manuscript has been created by the University of Chicago as Operator of Argonne National Laboratory ("Argonne") under Contract No. W-31-109-ENG-38 with the U.S. Department of Energy. The Korean side work was supported by the funds provided by the Ministry of Science and Technology of Korea (Project ID: 02-B03-00-003-1-0).

References

1) D. P. Weber, T. Sofu, P. A. Pfeiffer, W. S. Yang, T. A. Taiwo (ANL), H. G. Joo, J. Y. Cho, K. S. Kim, T. H. Chun (KAERI), T. J. Downar, J. W. Thomas, Z. Zhong (Purdue University), C. H. Kim (Seoul National University), The Numerical Nuclear Reactor for High Fidelity Integrated Simulation of Neutronic, Thermal-Hydraulic and Thermo Mechanical Phenomena, PHYSOR 2004, Chicago, IL, April 25-29, 2004.
2) D. P. Weber, T. A. Taiwo, W. S. Yang, P. A. Pfeiffer, P. H. Froehle, C. P. Tzanos, J. E. Cahalan, T. Sofu, Integrated 3-D Simulation Of Neutronic, Thermal-Hydraulic And Thermo-Mechanical Phenomena, The 10th International Topical Meeting on Nuclear Reactor Thermal Hydraulics (NURETH-10) Seoul, Korea, October 5-9, 2003.
3) J. W. Thomas, Z. Zhong, T. J. Downar (Purdue University), T. Sofu (ANL), Methodology for Coupling Computational Fluid Dynamics and Integral Transport Neutronics, PHYSOR 2004, Chicago, IL, April 25-29, 2004.
4) J.W. Thomas, H.C. Lee, T. J. Downar , Purdue University, T. Sofu, D. P. Weber**,** Argonne National Laboratory, H. G. Joo, J. Y. Cho, Korean Atomic Energy Research Institute, The Coupling Of The Star-Cd Software To A Whole-Core Neutron Transport Code Decart For PWR Applications," Proc. of Intl. Conf. on Supercomputing in Nuclear Applications, SNA'03, Paris, France, September 22-24, 2003.
5) STAR-CD, Version 3.150A, CD-Adapco Group, Melville, NY.
6) CFD.-ACE, CFD Research Corporation, Huntsville, Alabama.
7) T. Takeda, K. Ohya, E. Saji, Doppler Reactivity Calculation for Thermal Reactor Cells by Space-Dependent Multiband Method, J. Nucl. Sci. Technol, Vol. 33, 604, 1996.
8) D. P. Weber, et al., High-Fidelity Thermal-Hydraulic Analysis Using CFD and Massively Parallel Computers, 4th Intl. Conf. on Supercomputing in Nuclear Applications, SNA-2000, Tokyo, Japan, September 2000.
9) EPRI-NP-2511-CCM, Mathematical Modeling, Vol. 1: VIPRE-01, A Thermal-Hydraulic Analysis Code for Reactor Cores, Electric Power Research Institute, Palo Alto, California, Prepared by Battelle, Pacific Northwest Laboratories, Richland, Washington, November 1983.
10) Young, M. Y. and Secker, J. R., The Effect of Corrosion Product Deposition on Fuel Management, Advances in Nuclear Fuel Management III, October 2003.